ACS APPLIED MATERIALS & INTERFACES

RESEARCH ARTICLE

www.acsami.org

Giant Phase Transition Properties at Terahertz Range in VO_2 films Deposited by Sol–Gel Method

Qiwu Shi,[†] Wanxia Huang,[*,†] Yaxin Zhang,[‡] Jiazhen Yan,[†] Yubo Zhang,[†] Mao Mao,[†] Yang Zhang,[†] and Mingjing Tu[†]

[†]College of Materials Science and Engineering, Sichuan University, Chengdu, 610064, China

[‡]School of Physical Electronics, University of Electronic Science and Technology of China, Chengdu, 610054, China

Supporting Information

ABSTRACT: VO_2 films were fabricated on high-purity single-crystalline silicon substrate by the sol–gel method, followed by rapid annealing. The composition and microstructure of the films were investigated by X-ray photoelectron spectroscopy (XPS), X-ray diffraction (XRD), field-emission scanning electron microscopy (FE-SEM), and atomic force microscopy (AFM). The results indicated a polycrystalline nature with high crystallinity and compact nanostructure for the films, and the concentration of +4 valence vanadium is 79.85%. Correlated with these, a giant transmission modulation ratio about 81% of the film was observed by terahertz time domain spectroscopy. The experimentally observed transmission characteristics were reproduced approximately, by a simulation at different conductivities across the phase transition. According to the effective-medium theory, we assumed that it is important to increase the concentration of +4 valence vanadium oxide phases and improve the compactness of the VO_2 films for giant phase transition properties. The sol–gel-derived VO_2 films with giant phase transition properties at terahertz range, and the study on their composition and microstructure, provide considerable insight into the fabrication of VO_2 films for the application in THz modulation devices.

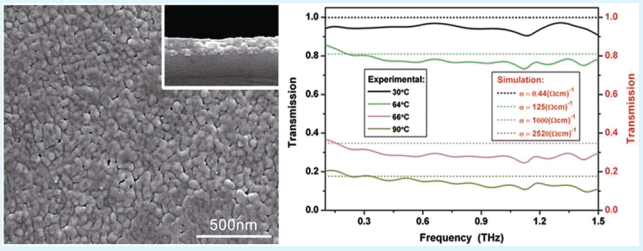

KEYWORDS: vanadium dioxide, thin film, phase transformation, terahertz transmission

INTRODUCTION

Vanadium dioxide (VO_2) is an interesting electron material that exhibits a reversible first order phase transition from a low temperature semiconductor phase to a high temperature metal phase at a critical temperature nearly 68 °C, which can be manipulated to a comfortable temperature by doping or stress.[1,2] The phase transition could be triggered by not only temperature, but also electric field, light, and pressure,[3−5] accompanied by abrupt several-orders-of-magnitude changes in optical and electrical properties.[6,7] All these properties make VO_2 a promising candidate for a variety of applications, such as thermochromic windows, infrared uncooled bolometer, optical and electrical switching, sensor devices, modulator and memory devices.[8−13] However, previous research reflects major concerns on the preparation, phase transition properties and applications for VO_2 films at infrared range.[14−17] Especially, a progress in terahertz (THz) science has attracted considerable researches to explore a utilization of VO_2 films in this new field. The THz frequency range falls below the optical phonon resonances of VO_2, so it is suggested that the optical properties of the insulating and metallic phases of VO_2 are significantly different at THz frequency.[18] For instance, the insulating VO_2 is highly transparent for wavelength above 45 μm (bellow 6.7 THz), with very low loss mainly caused by low-density free carrier absorption.[19]

Present studies have been particularly focused on the application of VO_2 films in the THz devices such as switching and modulation. A combination of VO_2 films and metamaterials opens up huge potential for further applications.[20,21] Q. Y. Wen et al. proposed a THz metamaterial with VO_2 cut-wire resonators fabricated on glass substrate, exhibiting an amplitude modulation over 65% to the THz transmission.[21] Nonetheless, the modulation ratio defined by the changes of THz transmission should be enhanced greatly for successful application. A hybridization with metallic structures can be employed to enhance the modulation ratio. Hendry et al demonstrated enhancements of modulation depths by two to five times, through fabricating metallic subwavelength square hole array patterns on silicon surfaces.[22] Kyoung et al. recently reported on enormously increased switching ratio by using THz slot antennas with submicrometer widths.[23,24] But the preparation of VO_2 films with excellent phase transition properties is a basic foundation for this question. C. H. Chen et al. demonstrated more than 4-fold change in THz transmission during the phase transition of VO_2 films, because of an epitaxial structure on sapphire substrates, which was grown by a pulsed reactive magnetron sputtering method.[25] Similar work was also reported by Mandal et al.[26] Nevertheless, the phase transition properties of the VO_2 film are commonly determined by not only the crystal structure, but also the fraction of +4

Received: June 9, 2011
Accepted: August 24, 2011
Published: August 24, 2011

valence vanadium oxide phases, crystallinity, grain size, and compactness of the film.

In this study, we presented VO_2 thin films deposited by inorganic sol−gel method on high-purity single-crystal Si substrate, followed by rapid annealing. Here, the sol−gel method is regarded as a quite promising and important method because of its low cost, easy coating of large-scale surface, flexible control of film thickness, and many other advantages.[27−29] Moreover the high-purity Si has been demonstrated to be not only the most transparent but also the least dispersive medium in the terahertz region, and hence is especially applicable as substrate contacts in VO_2-based THz devices.[30,31] The Si substrate was pretreated with hydrophilic solution and obtained an improved hydrophilicity, which resulted in a better contact performance between the film and Si substrate. Composition and microstructure of the films were investigated, in order to interpret a giant change of THz transmission about 81% observed during the phase transition. The VO_2 film with such significant phase transition properties at THz range realized by the sol−gel method has rarely been reported. Furthermore, the suggested viewpoints to understand the correlation of the composition and microstructure of VO_2 film with its phase transition will ultimately lead to improvement in fabrication of VO_2 films for the application in THz modulation devices.

EXPERIMENTAL SECTION

Preparation of VO_2 Films by Sol−Gel Method. We prepared V_2O_5 sol using an inorganic method:[32] 10.0 g of V_2O_5 powder was placed in a crucible and heated to 800 °C for about 30 min, and then the molten V_2O_5 was poured into 300 mL deionized (DI) water at room temperature. After vigorous stirring for 2 h, a deep brownish sol was filtered. And the n-type single crystal Si (400) substrate (0.5 mm thickness, ~4000 Ω cm resistivity) was pretreated with ethyl alcohol and hydrophilic solution composed of mixture of concentrated H_2SO_4 and H_2O_2 with a ratio of 1:1, and rinsed with DI water, in order to remove some organic contaminations and improve the hydrophilicity of Si surface. The precursor films were deposited on Si substrate by dip coating method. Then the films were dried around 90 °C for 15 min to remove the residual moisture. Subsequent annealing was done in a furnace at 500 °C for 1.5 h in a static atmosphere of nitrogen, in order to favor further crystallization and reduce the V_2O_5 phase to be VO_2 phase.

Characterization. Stoichiometric of the films was measured by X-ray photoelectron spectroscopy (XPS) (Xsam 800, Kratos) with Mg Kα ($h\nu$ = 1253.6 eV) exciting source. Crystalline structure was determined by X-ray diffraction (XRD) (X' Pert, Philips) with 4 kW monochromatic Cu Kα (λ = 0.15406 nm) radiation source. The morphologies were studied by both of field emission scanning electron microscopy (FE-SEM) (Inspect F, FEI) with an accelerating voltage of 20 kV and atomic force microscopy (AFM) (Nanoscope Multimode APM, Vecco Instrument) with a tapping mode under ambient conditions. Electrical resistivity dependent on the temperature was measured by the conventional four-point probe method, combined with an electrically heated substrate holder. The THz transmission of the films in the 0.1−1.5 THz range was measured as a function of temperature, using a THz time domain spectroscopy (THz-TDS) system (Mai Tai Z-2, Ti:sapphire laser, 70 kHz repetition rate and 110 V bias voltage).

RESULTS AND DISCUSSION

The wide-range survey XPS spectrum of the VO_2 film at Si substrates is displayed in Figure 1a. It reveals the presence of vanadium, oxygen, silicon, and carbon, where the silicon signals

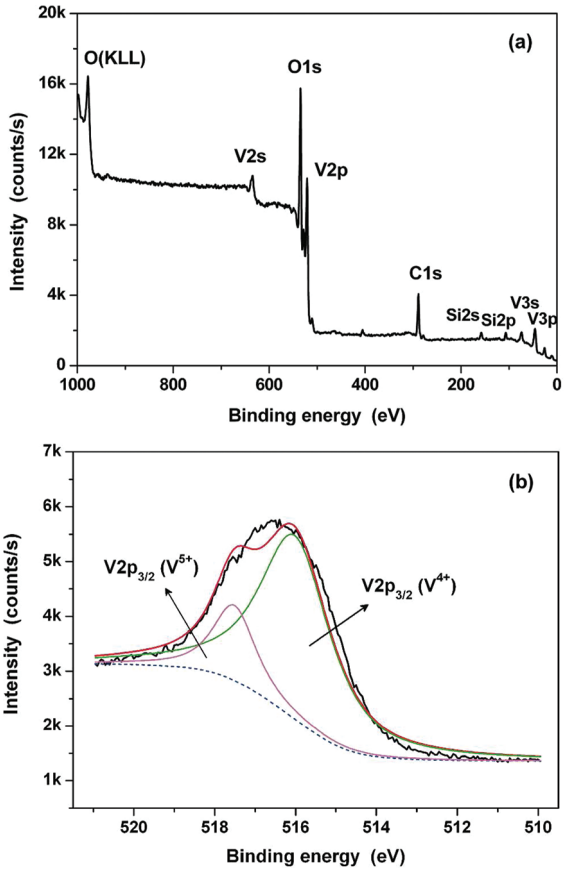

Figure 1. XPS spectrum of the VO_2 film on Si substrate: (a) Wide range survey of binding energy in XPS. (b) High-resolution scans of the V2p for the sample.

come from the substrates, and the carbon is attributed to surface contaminant. The high resolution scan of the V2p core levels was performed in Figure 1b, in which the peak position of V2p3/2 was fitted using a Shirley function with software XPS peak 4.1. Two valence states of vanadium were detected, +4 valence with a binding energy of 516.2 eV and +5 valence with a binding energy of 517.2 eV. Both of the binding energy for the two valence states of vanadium were in agree with the reported researches.[33,34] To obtain the relative concentrations of atoms in a homogeneous system, one simply divides each atom's peak intensity by its sensitivity factor and takes the ratio, giving the general relation[35,36]

$$\frac{n_A}{n_B} = \frac{I_A}{I_B}\frac{S_B}{S_A} \quad (1)$$

Where I is the peak intensity of atom, S is the sensitivity factor, and n is the atomic concentration, respectively.

According to it, the concentrations of the vanadium with different valence states were determined by calculating from the following equations

$$n_{V^{4+}} = \frac{I_{V^{4+}}S_{V^{5+}}}{I_{V^{4+}}S_{V^{5+}} + I_{V^{5+}}S_{V^{4+}}} \quad (2)$$

$$n_{V^{5+}} = \frac{I_{V^{5+}}S_{V^{4+}}}{I_{V^{4+}}S_{V^{5+}} + I_{V^{5+}}S_{V^{4+}}} \quad (3)$$

Noting that the S values for both of the two valences have been taken as the same as a standard (S = 1).[37] Finally, the +4 and +5

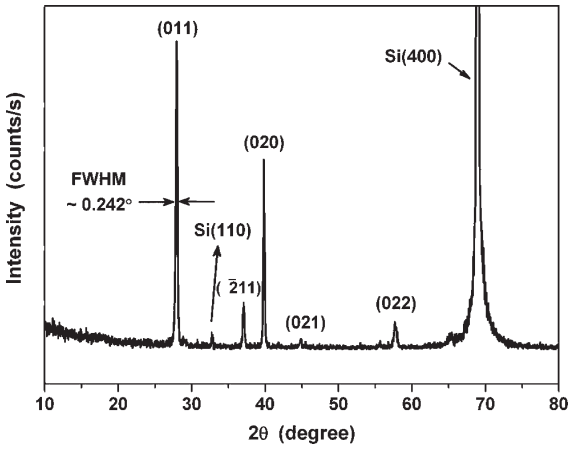

Figure 2. XRD patterns of the VO_2 films on Si (400) substrate.

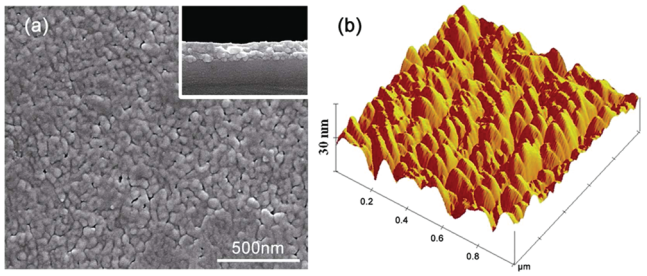

Figure 3. (a) FE-SEM image for films that were annealed at 500 for 1.5 h, the film consist of homogeneous and continuous nanoparticles, which is compact without obvious pore; inset: cross-section shape of the film. (b) AFM photograph for the presented sample.

valence were evaluated with the fractional percentages of 79.85 and 20.15%, respectively.

To investigate the crystal structure of the VO_2 film, a typical XRD pattern is studied here in Figure 2. A strong peak at 2θ = 68.83° is indexed to the diffraction from the Si (400) substrate, another weak peak at 2θ = 32.79° could be identified as the (110) edge orientation of Si substrate. The peaks at 2θ = 27.98, 36.98, 39.71, 44.65, and 57.42° correspond to (011), ($\bar{2}$11), (020), (021), and (022) planes of VO_2 phase, respectively. Although the (011) peak is strong, several other orientations are observed, indicating a polycrystalline nature. It could be explained by a weaker preferring orientation in thicker film.[38] However, the full width at half-maximum (fwhm) of the (011) peak is narrow with a value of 0.242, implying slightly better crystallinity of the film than the commonly reported results.[39]

Figure 3a shows an FE-SEM image of VO_2 film, which reveals the sample consisting of homogeneous and continuous nanoparticles. The size of the particles ranges from 50 to 90 nm with a mean value of about 60 nm. Moreover, the film is compact without obvious pore. It could be also seen in the AFM micrograph that the VO_2 film deposited on the single crystal Si substrate has compact nanostructure (Figure 3b). However, we can find some smaller grains growing in the interstitial of the larger grains, which would favor the improvement of the films' compactness. This special microstructure may give benefits to the change of optical properties during the phase transition of VO_2 films. A cross-section shape was observed insetting in the Figure 3a, displaying the thickness of about 220 nm. This

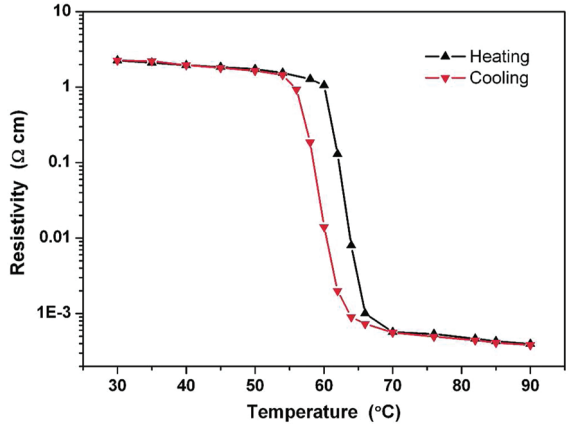

Figure 4. Hysteresis loop of the resistivity against temperature for the VO_2 film across the phase transition.

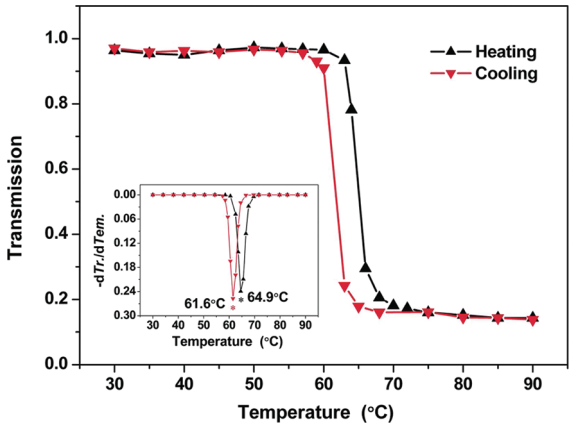

Figure 5. Hysteresis loop of the normalized transmission against temperature for the VO_2 film at 0.65 THz. Inset: the derivative of the transmission for the heating (black) and cooling transition curves (red).

thickness is suitable for fabricating VO_2 based metamaterial structures.

The electrical phase transition property of VO_2 film was studied by the four-point probe method to record variations in resistivity with temperature (Figure 4). Upon heating, the resistivity of the sample has an abrupt drop from 2.27 Ω cm at 30 °C to 3.97 × 10^{-4} Ω cm at 90 °C. The resistivity switching of the VO_2 film is nearly 4 orders of magnitude when cycled through the phase transition. This variation is also larger than the usually obtained change of 2−3 orders of VO_2 films, indicating competitive quality of VO_2 films fabricated on Si substrates by sol−gel process in our previous work.

The optical properties of the VO_2 film at THz range were investigated in the temperature range from 30−90 °C. The THz signals transmitted trough the film on the Si substrate was normalized by being compared to the THz signals transmitted through the bare substrate. Figure 5 displays a typical hysteresis loop of the normalized transmission amplitude against temperature for the VO_2 film at a selected frequency, 0.65 THz. When the film is in the semiconductor state, the THz transmission is almost 96%, for the pure VO_2 film and high-purity Si substrate are both essentially transparent in the 0.1−1.5 THz. However, as the temperature increases, the VO_2 transforms into a metallic state

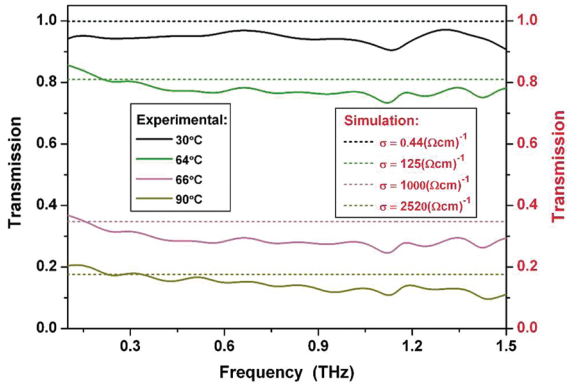

Figure 6. Comparison of the experimental and simulation transmission of the VO_2 film across the phase transition.

with a decrease of transmission to a minimum of 15%, due to the increased absorption and reflection loss of the film. The giant transmission modulation ratio about 81% at terahertz range for pure VO_2 film is significant for VO_2-based THz modulation devices.

Besides the giant transition, the derivative of the temperature dependence of transmission (−dTr/dTemp) was extracted with the Gaussian fit model. As shown in the Figure 5 inset, the phase transition temperature could be evaluated to be 64.9 °C in the heating transition and 61.6 °C in the cooling transition. The obvious decrease in transition temperature and hysteresis width of the VO_2 film has always been attributed to either the compressive strain along [011] direction, or larger fraction of +4 valence vanadium.[39] The decrease in transition temperature could also be caused by a size-induced modification as introduced by S. H. Chen.[40]

A simulation transmission of the VO_2 film at different conductivities across the phase transition was performed with a CST MICROWAVE STUDIO, in which the simplified expression for the ratio of the THz transmitted through a film to a bare substrate is as follows[41−43]

$$\frac{E_{\text{substrate+film}}}{E_{\text{substrate}}} = \frac{1 + n_{\text{substrate}}}{1 + n_{\text{substrate}} + Z_0\tilde{\sigma}}(\omega)d \qquad (4)$$

Where $n_{\text{substrate}}$ = 3.418 is the nearly frequency-independent index of refraction of the Si substrate, Z_0 = 377 Ω is the impedance of free space, d is the thickness of the VO_2 film, and $\tilde{\sigma}(\omega) = \sigma_1 + i\sigma_2$ is the complex conductivity of the film.

For a simulation correlated with the real conductivity of the VO_2 films that have been deduced by the resistivity measured directly, we assumed a purely real and frequency-independent electrical conductivity, $\tilde{\sigma}(\omega) = \sigma_{\text{dc}}$. The conductivities were selected at 0.44, 125, 1000, and 2520 $(\Omega\ \text{cm})^{-1}$, which corresponded to featured temperatures, at 30, 62, 66, and 90 °C. Accordingly, the comparison of the experimental and simulation transmission of the VO_2 film across the phase transition is shown in Figure 6. Although slight deviations exist, it can be seen that the simulation varying conductivities reproduce the experimentally observed transmission characteristics approximately, proving nearly 4 orders variation in conductivity of the film during the phase transition. It should be noted that these deviations may be attributed to either the loss of imaginary part of the conductivities in our calculation, or a measurement error in the resistivity against temperature. Although Thoman et al observed that the imaginary parts and the real parts of the conductivity had nearly the same absolute value for VO_2 film at different temperatures,[44] Mandal and Cocker et al measured the imaginary parts with very small absolute values which were far less than the real parts.[26,45] So how much the imaginary parts of conductivity can contribute to the transmittance should be further investigated.

The phase transition in VO_2 films occurs by gradual growth of metallic domains according to the commonly used effective−medium theory (EMT). But it has been suggested that the phase transition remains incomplete even at temperatures significantly above the transition point. Jepsen et al suggested two possible explanations for it: first, the formation of a uniform metallic phase is not complete; second, there is a small void fraction in the film.[46] We assume that the coexisting of +4 valence and +5 valence state in the VO_2 films is responsible for the incomplete formation of a uniform metallic phase. It is generally identified that a metal−insulator transition (MIT) does not occur in vanadium pentoxide (V_2O_5). Although recent experimental results show that the V_2O_5 film undergoes a MIT without a structural phase transition near 280 °C,[47] the existing +5 valence state in the VO_2 films will remain an insulating state at our experimental temperatures from 30 to 90 °C. The coexistence of the insulating and metallic phases in VO_2 films over a finite temperature range in the transition region has already been observed by mid-infrared near-field images and spatial maps of the X-ray diffraction intensity,[48,49] which may be due to the existence of other valence states of vanadium in the films. Furthermore, the void fraction is affected by the compactness of the film indirectly. Although our results indicate giant phase transition properties of VO_2 films at THz range, there is still some margin of improvement by increasing the concentration of +4 valence vanadium oxide phases and improving the compactness of the VO_2 films.

CONCLUSIONS

In conclusion, we have deposited 220 nm thick VO_2 film by inorganic sol−gel method on high-purity Si (400) substrate. The studies on composition and microstructure of the films indicate a polycrystalline nature with high crystallinity and compact nanostructure, the concentration of +4 valence vanadium is 79.85%. The resistivity switching of the VO_2 film is nearly 4 orders of magnitude when cycled through the phase transition. And a giant transmission modulation ratio about 81% was observed by THz-TDS, with a phase transition temperature evaluated to be 64.9 °C in the heating transition and 61.6 °C in the cooling transition. A simulation transmission of the VO_2 films at different conductivities across the phase transition has been performed, of which result reproduces the experimentally observed transmission characteristics approximately. It suggests that the phase transition properties of VO_2 films at THz range have a strong correlation with the fraction of +4 valence vanadium oxide phases and compactness of the films.

ASSOCIATED CONTENT

Supporting Information. An illustration for a hydrophilic treatment of the Si substrate and a supplement for the terahertz transmission data of the VO_2 film measured by THz-TDS. This material is available free of charge via the Internet at http://pubs.acs.org.

AUTHOR INFORMATION

Corresponding Author

*E-mail: huangwanxiascu@yahoo.com.cn. Tel/Fax: +86-28-8540-5781.

ACKNOWLEDGMENT

This work was financial supported by the National Natural Science Foundation of China (Grants 61072036 and 61001031), and the National Key Program of Fundamental Research of China (Grants 2007CB310401). We thank Analytical & Testing center of Sichuan University for their XRD analysis.

REFERENCES

(1) Manning, T. D.; Parkin, I. P.; Pemble, M. E.; Sheel, D.; Vernardou, D. *Chem. Mater.* **2006**, *16*, 744–749.
(2) Muraoka, Y.; Ueda, Y.; Hiroi, Z. *J. Phys. Chem. Solids* **2002**, *63*, 965–967.
(3) Kim, H. T.; Chae, B. G.; Youn, D. H.; Kim, G.; Kang, K. Y.; Lee, S. J.; Kim, K.; Lim, Y. S. *Appl. Phys. Lett.* **2005**, *86*, 242101.
(4) Cavalleri, A.; Tóth, Cs.; Siders, C. W.; Squier, J. A.; Ráksi, F.; Forget, P.; Kieffer, J. C. *Phys. Rev. Lett.* **2001**, *87*, 237401.
(5) Cao, J.; Ertekin, E.; Srinivasan, V.; Fan, W.; Huang, S.; Zheng, H.; Yim, J. W. L.; Khanal, D. R.; Ogletree, D. F.; Grossmanan, J. C.; Wu, J. *Nat. Nanotechnol.* **2009**, *4*, 732–737.
(6) Lappalainen, J.; Heinilehto, S.; Jantunen, H.; Lantto, V. *J. Electroceram.* **2008**, *22*, 73–77.
(7) Morin, F. J. *Phys. Rev. Lett.* **1959**, *3*, 34–36.
(8) Manning, T. D.; Parkin, I. P. *J. Mater. Chem.* **2004**, *14*, 2554–2559.
(9) Viswanath, B.; Ko, C.; Ramanathan, S. *Scr. Mater.* **2001**, *64*, 490–492.
(10) Huang, W. X.; Yin, X. G.; Huang, C. P.; Wang, Q. J.; Miao, T. F.; Zhu, Y. Y. *Appl. Phys. Lett.* **2010**, *96*, 261908.
(11) Messaoud, T. B.; Landry, G.; Gariépy, J. P.; Ramamoorthy, B.; Ashrit, P. V.; Haché, A. *Opt. Commun.* **2008**, *281*, 6024–6027.
(12) Driscoll, T.; Palit, S.; Qazilbash, M. M.; Brehm., M.; Keilmann, F.; Chae, B. G.; Yun, S. J; Kim, H. T.; Cho, S. Y.; Marie Jokerst, N.; Smith, D. R.; Basov, D. N. *Appl. Phys. Lett.* **2008**, *93*, 024101.
(13) Driscoll, T.; Kim, H. T.; Chae, B. G.; Kim, B. J.; Lee, Y. W.; Jokerst, N. M.; Palit, S.; Smith, D. R.; Ventra, M. D.; Basov, D. N. *Science* **2009**, *325*, 1518–1521.
(14) Wang, H. C.; Yi, X. J.; Li, Y. *Opt. Commun.* **2005**, *256*, 305–309.
(15) Rozen, J.; Lopez, R.; Haglund, R. F.; Feldman, L. C. *Appl. Phys. Lett.* **2006**, *88*, 081902.
(16) Suh, J. Y.; Donev, E. U.; Lopez, R.; Feldman, L. C.; Haglun, R. F. *Appl. Phys. Lett.* **2006**, *88*, 133115.
(17) Lee, K. W.; Kweon, J. J.; Lee, C. E.; Gedanken, A.; Ganesan, R. *Appl. Phys. Lett.* **2010**, *96*, 243111.
(18) Zhan, H.; Astley, V.; Hvasta, M.; Deibel, J. A.; Mittleman, D. M.; Kim, Y.-S. *Appl. Phys. Lett.* **2007**, *91*, 162110.
(19) Chen, C.; Zhou, Z. *Appl. Phys. Lett.* **2007**, *91*, 011107.
(20) Kyoung, J. S.; Seo, M. A.; Koo, S. M.; Park, H. R.; Kim, H. S.; Kim, B. J.; Kim, H. T.; Park, N. K.; Kim, D. S.; Ahn, K. J. *Phys. Status Solidi C* **2011**, *4*, 1227–1230.
(21) Wen, Q. Y.; Zhang, H. W.; Yang, Q. H.; Xie, Y. S.; Chen, K.; Liu, Y. L. *Appl. Phys. Lett.* **2010**, *97*, 021111.
(22) Hendry, E.; Lockyear, M. J.; Rivas, J. G.; Kuipers, L.; Bonm, M. *Phys. Rev. B* **2007**, *75*, 235305.
(23) Kyoung, J.; Seo, M.; Park, H.; Koo, S.; Sun, K. H.; Park, Y.; Kim, B.-J.; Ahn, K.; Park, N.; Kim, H.-T.; Kim, D.-S. *Opt. Exp.* **2010**, *18*, 16452.
(24) Seo, M.; Kyoung, J.; Park, H.; Koo, S.; Sun, K. H.; Bernien, H.; Kim, B.-J.; Cheo, J. H.; Ahn, Y. H.; Kim, H.-T.; Park, N.; Park, Q. H.; Ahn, K.; Kim, D.-S. *Nano Lett.* **2010**, *10*, 2064–2068.
(25) Chen, C. H.; Zhu, Y. H.; Zhao, Y.; Lee, J. H.; Wang, H. Y.; Bernussi, A.; Holtz, M.; Fan, Z. Y. *Appl. Phys. Lett.* **2010**, *97*, 211905.
(26) Mandal, P.; Speck, A.; Ko, C.; Ramanathan, S. *Opt. Lett.* **2011**, *36*, 1927–1929.
(27) Partlow, D. P.; Gurkovich, S. R.; Radford, K. C.; Denes, L. J. *J. Appl. Phys.* **1991**, *70*, 443–452.
(28) Ozer, N. *Thin Solid Films* **1997**, *305*, 80–87.
(29) Ningyi, Y.; Jinhua, L.; Chenglu, L. *Appl. Surf. Sci.* **2002**, *191*, 176–180.
(30) Dai, J. M.; Zhang, J. Q.; Zhang, W. L.; Grischkowsky, D. *J. Opt. Soc. Am. B* **2004**, *21*, 1379–1386.
(31) Jeon, T. I.; Grischkowsky, D. *Phys. Rev. Lett.* **1997**, *78*, 1106–1109.
(32) Yan, J. Z.; Zhang, Y.; Huang, W. X.; Tu, M. J. *Thin Solid Films* **2008**, *516*, 8554–8558.
(33) Zhang, Z. T.; Gao, Y. F.; Chen, Z.; Du, J.; Cao, C. X.; Kang, L.; Luo, H. *Langmuir* **2010**, *26*, 10738–10744.
(34) Alov, N.; Kutsko, D.; Spirovova, I.; Bastl, Z. *Surf. Sci.* **2006**, *600*, 1628–1631.
(35) Bowen Katarl, J. E.; Colvin, V. L.; Alivisatos, A. P. *J. Phys. Chem.* **1994**, *98*, 4109–4117.
(36) Jablonski, A. *Surf. Sci.* **2009**, *603*, 1342–1352.
(37) Wagner, C. D.; Davis, L. E.; Zeller, M. V.; Taylor, J. A.; Raymond, R. H.; Gale, L. H. *Surf. Interface Anal.* **1981**, *3*, 211–225.
(38) Balu, R.; Ashrit, P. V. *Appl. Phys. Lett.* **2008**, *92*, 021904.
(39) Yang, Z.; Ko, C.; Ramanathan, S. *J. Appl. Phys.* **2010**, *107*, 053514.
(40) Chen, S. H.; Ma, H.; Dai, J.; Yi, X. J. *Appl. Phys. Lett.* **2007**, *90*, 101117.
(41) Tu, J. J.; Homes, C. C.; Strongin, M. *Phys. Rev. Lett.* **2003**, *90*, 017402.
(42) Tinkham, M. *Phys. Rev.* **1956**, *104*, 845–846.
(43) Walther, M.; Cooke, D. G.; Sherstan, C.; Hajar, M.; Freeman, M. R.; Hegmann, F. A. *Phys. Rev. B* **2007**, *76*, 125408.
(44) Thoman, A. *Far-Infrared Probing of the Metal-Insulator Transition in Thin-Films and of the Dynamics of Pure Ionic Liquids: An Application of THz Time-Domain Spectroscopy*; Universitatsbibliothek: Freiburg, Germany, 2009; pp 82−96.
(45) Cocker, T. L.; Titova, L. V.; Fourmaux, S.; Bandulet, H.-C.; Brassard, D.; Kieffer, J.-C.; EI Khakani, M. A.; Hegmann, F. A. *Appl. Phys. Lett.* **2010**, *97*, 221905.
(46) Jepsen, P. U.; Fischer, B. M.; Thoman, A.; Helm, H.; Suh, J. Y.; Lopez, R.; Haglund, R. F. *Phys. Rew. B* **2006**, *74*, 205103.
(47) Kang, M.; Kim, I.; Kim, S. W.; Ryu, J. W.; Park, H. Y. *Appl. Phys. Lett.* **2011**, *98*, 131907.
(48) Qazilbash, M. M.; Brehm, M.; Chae, B. G.; Ho, P.-C.; Andreev, G. O.; Kim, B. J.; Yun, S. J.; Balatsky, A. V.; Maple, M. B.; Keilmann, F.; Kim, H. T.; Basov, D. N. *Science* **2007**, *318*, 1750–1753.
(49) Qazilbash, M. M.; Tripathi, A.; Schafgans, A. A.; Kim, B. J.; Kim, H. T.; Cai, Z. H.; Holt, M. V.; Maser, J. M.; Keilmann, F.; Shpyrko, O. G.; Basov, D. N. *Phys. Rev. B* **2011**, *83*, 165108.